

Expanding the Synthesis Field of High-Silica Zeolites

Diandian Shi, Kok-Giap Haw, Cassandre Kouvatas, Lingxue Tang, Yiyang Zhang, Qianrong Fang, Shilun Qiu, Valentin Valtchev

► **To cite this version:**

Diandian Shi, Kok-Giap Haw, Cassandre Kouvatas, Lingxue Tang, Yiyang Zhang, et al.. Expanding the Synthesis Field of High-Silica Zeolites. *Angewandte Chemie International Edition*, Wiley-VCH Verlag, 2020, 59 (44), pp.19576-19581. 10.1002/anie.202007514 . hal-03040578

HAL Id: hal-03040578

<https://hal-normandie-univ.archives-ouvertes.fr/hal-03040578>

Submitted on 4 Dec 2020

HAL is a multi-disciplinary open access archive for the deposit and dissemination of scientific research documents, whether they are published or not. The documents may come from teaching and research institutions in France or abroad, or from public or private research centers.

L'archive ouverte pluridisciplinaire **HAL**, est destinée au dépôt et à la diffusion de documents scientifiques de niveau recherche, publiés ou non, émanant des établissements d'enseignement et de recherche français ou étrangers, des laboratoires publics ou privés.

Expanding the synthesis field of high silica zeolites

Diandian Shi,^[a] Kok-Giap Haw,^[a] Cassandre Kouvatat,^[b] Lingxue Tang,^[a] Yiyang Zhang,^[a] Qianrong Fang,^[a] Shilun Qiu,^[a] Valentin Valtchev^{*[b,c]}

Abstract: Aluminosilicate zeolites are synthesized under hydrothermal conditions in basic/alkaline medium in the pH range between 9 and 14. Here we report the synthesis of MFI-type zeolite in acidic medium. The critical parameter determining the zeolite formation in acidic medium was found to be the isoelectric point (IEP) of gel particles. MFI-type zeolite was synthesized above the isoelectric point of the employed silica source, where the silica species exhibit a negative charge and the paradigm of zeolite formation based on the electrostatic interaction with the positively charged template is retained. No zeolite formation is observed below the isoelectric point of silica. The impact of aluminum on the zeolite formation is also studied. The results of this study will serve to extend the zeolite synthesis field of high silica zeolites to acidic medium and thus open new opportunities to control the zeolite properties.

Zeolites are microporous aluminosilicate molecular sieves that have a variety of significant applications in catalysis, adsorption, separation and ion exchange.^[1] The intensive industrial use of zeolites is based on their unique properties as ordered channel systems containing active sites in a well-defined confine environment, which is the origin of their unraveled shape-selectivity, and molecular sieving properties.^[2]

In general, zeolites are synthesized under hydrothermal conditions in a basic medium where the OH⁻ is the mineralizing agent. The conventional zeolite syntheses are performed at relatively high pH (>9) using alkali metal and/or tetraalkylammonium cation as a structure-directing agent (SDA).^[3] Zeolites are also synthesized using F⁻ as a mineralizer. The synthesis in fluoride medium is usually performed under neutral conditions (pH = 6-8).^[4] The physicochemical properties of a zeolite obtained by the hydroxide and fluoride route differ substantially.^[5] Thus, both routes deserve attention, although the industrial syntheses are limited to the use of the hydroxide medium.

The synthesis in the basic medium was first developed, mimicking the zeolite formation in nature, namely the high-temperature hydrothermal conditions in pegmatites.^[6] These syntheses were performed at temperatures higher than 250 °C. In the late 50ies, Milton discovered that zeolites can be obtained under much lower temperatures using highly reactive alkaline aluminosilicate hydrogels.^[7] This synthesis mode, which is used in the industry, was further developed by Breck.^[8]

The fluoride medium synthesis of zeolites, pioneered by Flanigen and Patton in the late 1970s,^[9] was an important breakthrough diversifying the synthesis conditions and providing materials with different properties. Guth, Kessler, and co-workers further developed this synthetic route.^[10] This group systematically studied the zeolite formation in fluoride medium and synthesized different microporous materials, including aluminosilicates, aluminophosphates, and gallophosphates. The syntheses were performed in the pH range 5-9, and an attempt to obtain zeolite below pH = 5 was reported.^[11] However, the formation of zeolite at pH below 5 without using seeds was not achieved.

In the conventional basic/alkaline medium synthesis, the nucleation is abundant, and the crystals grow fast. Consequently, they contain a lot of intergrowths and a relatively large number

[a] D. Shi, Dr. K.-G. Haw, L. Tang, Y. Zhang, Prof. Q. Fang, Prof. S. Qiu
State Key Laboratory of Inorganic Synthesis and Preparative Chemistry, Jilin University, Changchun 130012, P. R. China

[b] Prof. V. Valtchev, Dr. C. Kouvatat
Normandie Univ, ENSICAEN, UNICAEN, CNRS, Laboratoire Catalyse et Spectrochimie, 6 Marechal Juin, 14050 Caen, France
E-mail: valentin.valtchev@ensicaen.fr

[c] Prof. V. Valtchev
Qingdao Institute of Bioenergy and Bioprocess Technology, Chinese Academy of Sciences, 189 Songling Road, Laoshan District, Qingdao, Shandong 266101, P. R. China

Supporting information for this article is available on the WWW under <http://www.angewandte.org> or from the author.

80 of framework defects.^[12] Under framework
81 defects, we refer missing T (tetrahedral) atoms
82 replaced by silanols. The presence of defects
83 silanols has a negative impact on zeolite catalytic
84 since it is a coke trap in the hydrocarbon
85 conversion.^[13] The silanols also decrease the
86 hydrophobicity of the all-silica zeolite
87 materials.^[14] Similar problems can be reduced to a
88 considerable extent by the synthesis in fluoride
89 medium where the crystals grow slowly, which
90 limits the number of defects. Bleken *et al.* showed
91 that the coke formation in ZSM-5 prepared via the
92 fluoride route is negligible with respect to the
93 hydroxide medium prepared counterpart.^[15] Thus,
94 the fluoride route has shown its most notable
95 advantage in producing zeolite crystals of fewer
96 framework defect sites.^[16] However, the zeolite
97 crystals synthesized in fluoride medium are
98 usually several tens of micrometers large and
99 impose diffusion limitations, which limits their
100 applications. On the other side, the fluoride
101 medium growth crystals are of great importance for
102 fundamental studies of zeolites. From a practical
103 point of view, the synthesis in fluoride medium
104 might present interest since the low pH might be
105 appropriate to incorporate transition metals in the
106 zeolite structure.^[17]

107 The objective of this work is to extend the
108 zeolite formation at the pH range below 5, i.e.,
109 under acidic conditions without the assistance of
110 seeds. This objective involves fundamental and
111 practical aspects since the results of the study will
112 provide valuable information about the critical
113 factors controlling zeolite formation and bring
114 more flexibility in the preparation of zeolite
115 materials with controlled properties.

116 It is well known that silica source plays an
117 important role in zeolite synthesis.^[18] Using
118 different silica sources may result in changing the
119 crystallization pathway and even in the formation
120 of an undesired crystalline phase. The preliminary
121 work on the optimization of gel composition aimed at
122 reaching a successful synthesis of the zeolite was
123 performed with pyrogen silica known as fumed
124 silica. We selected this silica source since it was
125 previously used in the fluoride medium synthesis
126 of zeolites.^[10c] MFI-type zeolite was obtained
127 from a gel with molar composition $1.0 \text{ SiO}_2 : 0.37$
128 $\text{TPABr} : 0.00167 \text{ Al}_2\text{O}_3 : x \text{ HF} : y \text{ NH}_4\text{F} : 40.78$
129 H_2O , where x and y were varied to control the pH.

The details on synthesis can be found in the
Supporting Information. Using a gel composition
with $\text{Si}/\text{Al} = 300$, highly crystalline MFI-type
material was obtained at $\text{pH} = 5.0, 3.6,$ and 2.3
(Figure 1). The synthesis with a gel with an initial
 pH of 2.3 and $\text{Si}/\text{Al} = 300$ was reproduced using
tetraethylorthosilicate (TEOS), colloidal silica
(Ludox AS-40), and silicic acid as silica sources.
The pH of the mother liquor after the synthesis
was measured. In all cases the pH was lower than
in the initial gel, but varied as a function of silica
source. Thus for fumed silica, TEOS, and silicic
acid the final pH was about 1.7 , while for the
colloidal silica 1.9 . The XRD patterns of the
samples synthesized from these silica sources are
presented in Figure S1. Thus using fumed silica,
TEOS, and Ludox AS-40 yielded pure and highly
crystalline MFI-type zeolite. Only traces of MFI
were observed in the synthesis with silicic acid.
Poor crystallinity of zeolite phase might be due to
the relatively large silica particles, which might
require much longer synthesis time (Figure S2e,f).
Nevertheless, this set of results proved that the
crystallization of zeolitic material in acidic
medium is possible. The SEM inspection showed
that all silica sources yielded MFI-type crystals
with the typical coffin morphology (Figure S2).
The crystals range between 10 and $50 \mu\text{m}$ in size.
Ludox AS-40 synthesized material contains some
small particles, most probably amorphous,
covering the large zeolite crystals. No traces of
amorphous material were observed in the TEOS
synthesized sample. The amorphous phase, large
particles with random shape, dominated the
product obtained with silicic acid. A few but well-
shaped crystals with the characteristic of MFI-
type material features were observed in this
sample.

The incorporation of hetero elements in the
zeolite framework is indispensable for catalytic
applications, which is a major field of zeolite uses.
Therefore, the impact of aluminum on the zeolite
crystallization in acidic medium was studied. The
best result in terms of zeolite crystallinity was
obtained with fumed silica. Thus the synthesis of
Al-containing MFI-type material was performed
with this silica source. The crystal growth kinetics
of a gel with Si/Al ratio of 300 and relatively low
 pH (2.3) was studied and used as a reference for
the synthesis duration. The hydrothermal

180 treatment was performed at 160 °C. The first trace
 181 of MFI was observed after four days, and a fully
 182 crystalline material obtained after 13 days (Figure
 183 S3). This reference synthesis was used to calculate
 184 the zeolite yield, which was found to be 78 %,
 185 based on the silica plus alumina content in the
 186 initial gel. Consequently, all experiments related
 187 to the impact of aluminum on the zeolite
 188 formation under acidic conditions were performed
 189 at 160 °C for 13 days. The initial pH was 2.3 and
 190 the molar composition of the gel was 1.0 SiO₂ :
 191 0.3 TPABr : z Al₂O₃ : 0.36572 HF : 0.17124
 192 NH₄F : 40.6 H₂O, where z = 0.01, 0.005, 0.0033,
 193 0.00167, and 0, giving a Si/Al ratio of 50, 100,
 194 150, 300 and infinity (∞). The synthesized
 195 samples were denoted FS-50, FS-100, FS-150,
 196 FS-300, and FS-∞ as a function of the Si/Al ratio.
 197 The XRD patterns of the obtained products are
 198 depicted in Figure S4 and their relative
 199 crystallinity presented in Table 1.

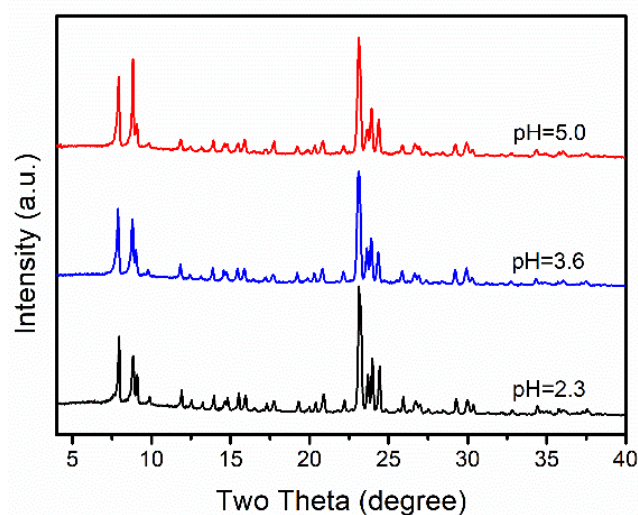


Figure 1. XRD pattern of the MFI-type samples synthesized from gels with different pH values at 160 °C for 13 days.

Table 1. Physicochemical characteristics of the MFI-type samples synthesized from gels with pH = 2.3 and different Si/Al ratios at 160 °C for 13 days using fumed silica as a silica source.

Sample	Si/Al ratio		Crystallinity (%)	Weight loss (%)		S _{BET} m ² g ⁻¹	V _{micro} cm ³ g ⁻¹	V _{total} cm ³ g ⁻¹
	Initial gel	Crystalline product		25-300 (°C)	300-600 (°C)			
FS-∞	∞	∞	100	0.37	12.42	336	0.18	0.18
FS-300	300	375	100	0.49	12.45	392	0.17	0.18
FS-150	150	182	100	0.88	12.34	466	0.18	0.18
FS-100	100	113	63	1.20	7.51	253	0.11	0.14
FS-50	50	61	33	3.68	5.28	128	0.05	0.12

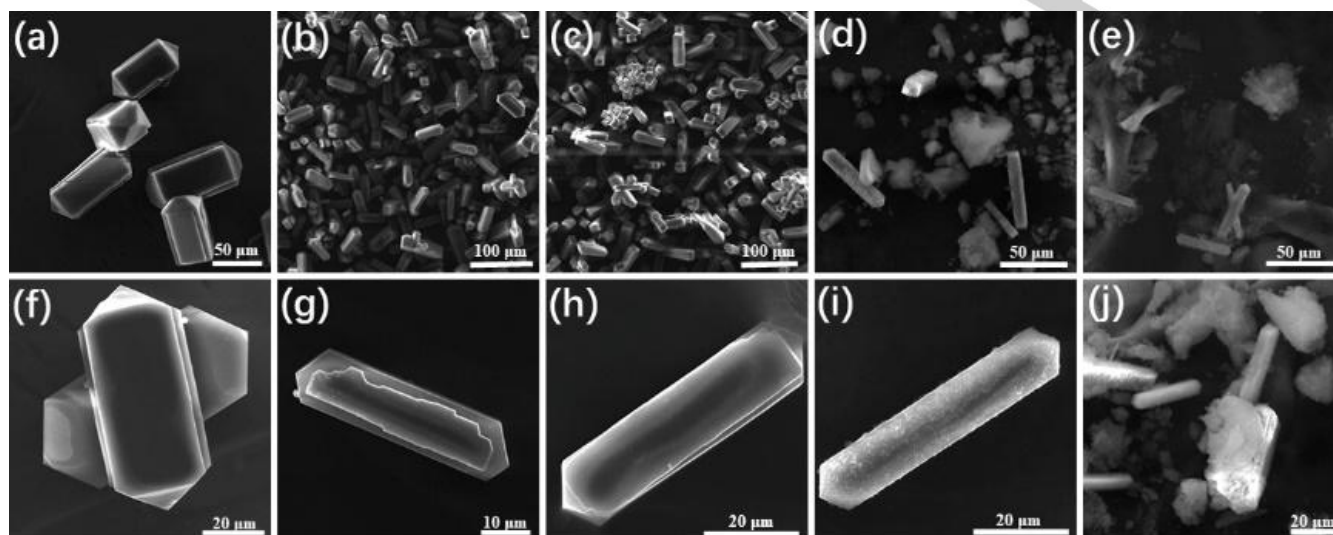
207
 208 Highly crystalline samples were obtained using
 209 gels with silicon to aluminum ratio higher than
 210 150. The crystallinity of the samples synthesized
 211 from gels with Si/Al ratio of 100 and 50 was
 212 lower. A closer look at their XRD patterns revealed
 213 the presence of an amorphous phase, i.e., a halo
 214 the 20-30° Two Theta range, for these two
 215 samples. The extension of the crystallization time
 216 to 18 days improved the crystallinity of FS-100
 217 (Figure S5) and FS-50 (Figure S6); yet some
 218 amorphous material was present in the solid. The
 219 SEM inspection confirmed that FS-∞, FS-300,
 220 and FS-150 are highly crystalline products (Figure
 221 2). The crystals are well-shaped with clean faces.
 222 No trace of other phase was observed. FS-100 and
 223 FS-50 contain crystals with the characteristic
 224 MFI-type material morphology. The crystals are
 225 covered with small particles that do not exhibit
 226 crystalline features. The amount of this phase
 227 which we consider amorphous due to the absence

228
 229 of XRD pattern, is larger in the FS-50 sample
 230 (Figure S6). The results of the SEM and XRD
 231 studies are in good agreement and confirm that a
 232 high concentration of Al is not favorable for the
 233 zeolite formation in acidic medium.

234
 235 The system yielding FS-300 was used to
 236 explore the pH range below 2 as the NH₄F was
 237 kept constant, and the content of HF was varied to
 238 control the pH. The formation of MFI-type zeolite
 239 was still possible at pH = 2, but the crystallinity of
 240 the sample obtained after 13 days of hydrothermal
 241 treatment was relatively low. The synthesis was
 242 extended to 18 days to get a highly crystalline
 243 product (Figure S7). Further decrease of the pH to
 244 1.5 resulted in amorphous solid after 13 days of
 245 hydrothermal treatment. The first traces of MFI-
 246 type material were observed after 23 days of
 247 crystallization (Figure S8), while the solid
 248 obtained after 33 days contained MFI-type
 material and amorphous. The crystallinity of the

249 zeolite phase was improved after 38 days 256
 250 crystallization, but new peaks in the 20 – 23° T₂₅₇
 251 Theta range appeared in the XRD pattern. These 258
 252 peaks reveal the co-crystallization of a dense non- 259
 253 zeolitic phase. The synthesis at pH = 1 did not 260
 254 yield MFI-type material after 40 days 261
 255 hydrothermal treatment.

The paradigm of zeolite formation is based on
 the electrostatic interactions between the
 positively charged templating species that remain
 in channels/cages of zeolite structure and
 negatively charged silica species that built up the
 framework. The surface charge of silica species



262
 263 **Figure 2.** SEM micrographs of the MFI-type materials synthesized from gels with different Si/Al ratios at 160 °C for 13 days. Low and high magnification images of
 264 FS-∞ (a, f), FS-300 (b, g), FS-150 (c, h), FS-100 (d, i), and FS-50 (e, j).

265 depends on the pH of the system. Therefore, 289
 266 have performed a zeta potential analysis^[19] 290
 267 evaluate how the pH influences the surface charge 291
 268 of fumed silica. The measurements were 292
 269 performed in the pH range 1 – 11, as each 293
 270 experiment was repeated ten times. Figure 294
 271 shows the zeta potential plot of the fumed silica 295
 272 a function of the pH value. The isoelectric point 296
 273 the employed fumed silica, where the surface 297
 274 charge of silica species is electrically neutral, was 298
 275 found to be in the pH range 2.0 – 2.2. 299
 276 The results of zeta potential measurements shed 300
 277 light on the crystallization behavior of MFI-type 301
 278 zeolite in acidic medium. The zeolite formation 302
 279 under acidic medium is possible solely at pH 303
 280 above the IEP of silica. With the decrease of 304
 281 pH and approaching the IEP of fumed silica 305
 282 zeolite formation is perturbed and even becomes 306
 283 impossible when the surface charge of silica 307
 284 species is inverted to positive, i.e., below the 308
 285 isoelectric point. In the system under investigation 309
 286 we have successfully synthesized MFI-type 310
 287 material at pH equal to 5, 3.6 and 2.3; the latter 311
 288 being relatively close to the isoelectric point of

fumed silica. The synthesis at a pH = 2, which is
 the IEP of the employed fumed silica, was still
 possible, but the time required to obtain a highly
 crystalline product was substantially extended. In
 the system with pH = 1.5, below but yet close to
 the IEP, only a part of the silica was converted
 into MFI-type material no matter the fact that the
 synthesis time was tripled. The last result might
 look surprising, but there is not a discrepancy in
 the experimental data. Namely, the surface charge
 in the IEP is considered neutral in the statistical
 mean. Close to the IEP there are still negatively
 charged silica species, which interact with the
 positively charged TPA⁺. These interactions,
 however, are strongly perturbed, which explain
 the decrease in the crystal growth rate and the
 partial conversion of silica into the zeolite. Only
 when the pH of the gel is substantially below the
 isoelectric point, and the charge of silica is fully
 inverted to positive the formation of zeolite is
 suppressed.

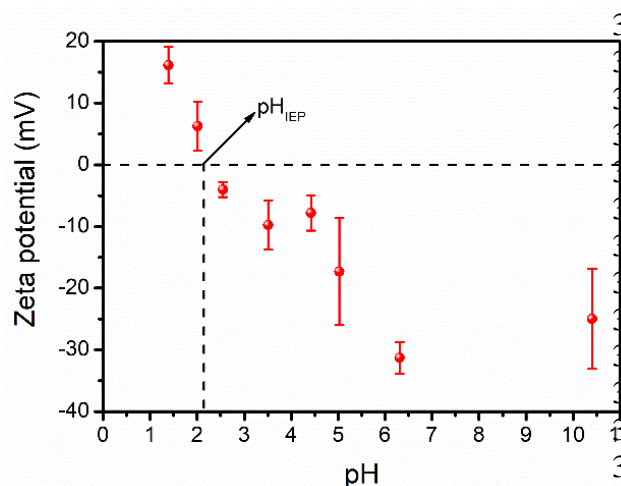


Figure 3. Zeta potential of fumed silica as a function of pH.

As reported above, the presence of Al in the initial gel has a negative impact on the zeolite formation under acidic medium. Only when the Si/Al ratio is above 150, i.e., when a few Al atoms were introduced in the initial gel, the MFI-type materials can be readily obtained. The crystallinity of the samples synthesized from the initial systems with Si/Al ratio of 100 and 50 was 63 and 33% respectively (Table 1). We attribute this result to the higher IEP of aluminum hydroxide, which is $\text{pH} = 7.7$.^[20] Thus the positively charged aluminum species exhibit repulsive interactions with the positively charged template. Thus zeolite formation is sensitive to the Si/Al ratio in acidic medium. This result shows that the incorporation of transition metals in the zeolite framework under acidic conditions will depend strongly on the isoelectric point of metal hydroxide.

The MFI-type materials were subjected to physicochemical characterization using complementary methods to evaluate the impact of the acidic medium on their properties. The crystallinity of materials was already discussed based on X-ray diffraction study. The short-range order was studied by comparing the ^{29}Si MAS NMR spectra of silicalite-1 synthesized in acidic medium (FS- ∞), and a counterpart synthesized in basic medium (Figure S9). The resonances observed in ^{29}Si MAS NMR correspond to quaternary Q $_n$ species, with $n = 1, 2, 3,$ or 4 stands for the number of another silicon atom directly connected to the Si atom concerned, through an oxygen bond (Si—O—Si). The two samples display resonances in the $[-107 \text{ ppm}; -120 \text{ ppm}]$

corresponding to Q $_4$ species (Figure 4). In contrast to the material synthesized in basic medium (Figure 4b), the FS- ∞ sample exhibits well-resolved peaks corresponding to Q $_4$ (Si—(OSi) $_4$) silicon species, reflecting different crystallographic T positions in MFI-structure (Figure 4a). The Q $_4$ resonances of the basic medium synthesized silicalite-1 (Figure 4b) are broader because of a less ordered three-dimensional Si—(OSi) $_4$ network. Also, a broad resonance at -103 ppm corresponding to Q $_3$ (Si—(OSi) $_3$ —OH) is observed. This is typical of a discontinuity between SiO $_4$ tetrahedra, leading to the formation of Si—OH bonds, and thus defect sites in the zeolite framework. However, no Q $_3$ is observed in the spectrum of FS- ∞ (Figure 4a), which is confirmed by the absence of signal enhancement in this region in the $^{29}\text{Si}\{1\text{H}\}$ CP MAS spectrum (Figure 4, inset). The last result unambiguously proves a lack of Si—OH defects in FS- ∞ , reinforcing the conclusion of a well-ordered 3D structure.

The FS- ∞ spectrum contains a broad peak at -125 ppm , which is not observed in the reference basic medium synthesized silicalite-1. This peak is attributed to the fluoride ions, which have certain mobility between SiO $_4/2$ tetrahedra. The large signal is thus typical of framework silicon sites that undergo dynamic exchange between 4- and 5-coordinated environments, due to fluoride ion mobility.^[21] Briefly, the silicalite-1 sample synthesized under acidic conditions exhibits the.

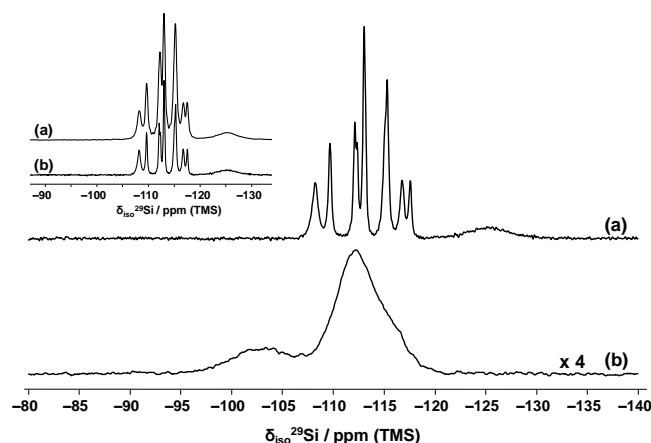


Figure 4. Weight normalized ^{29}Si MAS NMR spectra of as-synthesized silicalite-1 samples synthesized in (a) acidic (FS- ∞) and (b) basic medium. Inset: (a) $^{29}\text{Si}\{1\text{H}\}$ CPMAS and (b) ^{29}Si MAS NMR spectra of as synthesized silicalite-1 samples synthesized in acidic (FS- ∞) medium.

386 typical high ordering and absence of framework
387 defects characteristic for the synthesis in fluoride
388 medium

389 The incorporation of Al in zeolite framework
390 was studied by ^{27}Al MAS NMR on sample FS-
391 150. Figure S10 shows the spectra of zeolite
392 synthesized and calcined ZSM-5 sample
393 synthesized in acidic medium. Both samples
394 exhibit aluminum signal in the region of 55 ppm
395 corresponding to framework tetrahedral Al sites.
396 In the case of calcined sample (Figure S10) a
397 another resonance is observed at ≈ 0 ppm
398 corresponding to extraframework octahedral
399 aluminum species, which have left the
400 intraframework tetrahedral environment. The
401 broadening of this signal is due to a distribution
402 of Al^{VI} environment. The fraction of octahedral
403 was ca. 10 %.

404 The FS series of samples were subjected to
405 thermal analysis to evaluate template and water
406 content (Figure S11). The weight loss below
407 300 °C is attributed to water release, and the one
408 in the temperature range 300-600 °C to the
409 combustion of the TPA (Table 1). Highly
410 crystalline samples show negligible loss below
411 300 °C, which reveals their hydrophobic nature.
412 similar weight loss was observed in the high
413 temperature range corresponding to 4 TPA
414 molecules per unit cell. The samples that were not
415 fully crystalline (FS-100 and FS-50) showed
416 higher water content and lower template content.
417 Thus, there is a close correlation between the
418 crystallinity of the samples and the results of
419 thermal analysis.

420 The porosity and textural characteristics of the
421 FS series of samples were determined by nitrogen
422 (N_2) adsorption-desorption measurements at 77 K
423 (Figure S12). The N_2 sorption isotherms of highly
424 crystalline samples (FS- ∞ , FS-300, and FS-150)
425 displayed the typical type I isotherm
426 characteristic of microporous materials.^[22] These
427 samples exhibit a second small uptake with
428 hysteresis at about 0.1 P/P₀. Such additional
429 hysteresis has already been reported for silicalite
430 1.^[23] The most plausible explanation of this
431 feature is the orthorhombic – monoclinic phase
432 transition of the MFI-type framework.^[22, 24] The
433 micropore volume of these samples is 0.18 cm³g⁻¹,
434 which proves an excellent crystallinity. Lower
435 micropore volume was recorded for FS-100 and

FS-50, which is in line with the XRD analysis
(Table 1).

The set of the physicochemical analyses shows
that the properties of zeolites synthesized in an
acidic fluoride-containing medium are similar to
their counterparts obtained in a neutral medium
using fluoride as a mineralizer.

The set of experimental data shows that it is
possible to form a zeolite under acidic medium.
The critical factor determining the ability of
zeolite to crystallize under acidic conditions is the
isoelectric point of silica, i.e., the surface charge
of silica species. In the present case, the fumed
silica with IEP around two readily transformed
into MFI-type material in the pH range 2-5. Close
to the IEP, the zeolite synthesis was still possible,
but the crystallization rate slowed down, and only
partial transformation of the initial system into
zeolite was observed. Using a gel with pH below
the IEP did not yield a zeolitic material since the
surface charge of silica was reversed, which led to
repulsive interactions with the structure-directing
agent.

It should be noted the role of the F^- as
mineralizer that dissolves silica source and
transport the silica species to the structure
directing agent. The solubility of silica is limited
in most of mineral acids, which make them
unappropriate for zeolite synthesis. Thus the HF
acid and its derivatives are probably the sole
option for zeolite synthesis in acidic medium.

The aluminum incorporation in zeolite
framework is limited under acidic conditions,
which is a consequence of the high IEP of alumina
with respect to silica. Hence the introduction of
heteroatoms in zeolite structure will strongly
depend on their IEP, i.e., the surface charge of
their species in acidic medium.

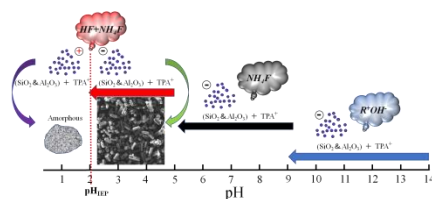
The present study opens the route to the acidic
medium synthesis of zeolites. This pioneering
work will have to be further deepened to reach a
practical perspective, as the first issues are the
incorporation of heteroatoms in the zeolite
framework and the decrease of the crystal size.
The recycling of fluoride effluent will be
necessary to make the process environmentally
benign.

- 484 **Acknowledgments** 531
- 485 V.V., S.Q. and Q.F. acknowledge the support 532
- 486 from the joint Sino-French international 533
- 487 laboratory "Zeolites". V.V. acknowledges the 534
- 488 talent start-up funding provided by QIBEBT. Q.F. 535
- 489 thanks the National Natural Science Foundation of 536
- 490 China (21571079, 21621001, 21390394, 537
- 491 21571076 and 21571078) for financial support. 538
- 492 **Keywords:** Acidic medium • Crystallization • MFI-type • Zeolites 539
- 493 [1] a) J. Y. Li, A. Corma, J. H. Yu, *Chem. Soc. Rev.* **2015**, *44*, 7112-7127; b) V. 540
- 494 Valtchev, L. Tosheva, *Chem. Rev.* **2013**, *113*, 6734-6760; c) C. Martínez, A. 541
- 495 Corma, *Coord. Chem. Rev.* **2011**, *255*, 1558-1580; d) S. Mintova, M. Jaber, V. 542
- 496 Valtchev, *Chem. Soc. Rev.* **2015**, *44*, 7207-7233. 543
- 497 [2] A. Khamkeaw, M. Phisalaphong, P. Jongsomjit, K. A. Lin, A. C. K. Yip, *Hazard. Mater.* **2019**, *384*, 121161. 544
- 498 [3] a) F. Dubray, S. Moldovan, C. Kouvatou, J. Grand, C. Aquino, N. Barrier, J. P. Gilson, N. Nesterenko, D. Minoux, S. Mintova, *J. Am. Chem. Soc.* **2019**, *141*, 8689-8693; b) M. Smaïhi, O. Barida, V. Valtchev, *Eur. J. Inorg. Chem.* **2003**, *2003*, 4370-4377; c) R. F. Lobo, S. L. Zones, M. E. Davis, *Journal of inclusion phenomena and molecular recognition in chemistry* **1995**, *21*, 47-78. 545
- 499 [4] P. Barrett, M. Cambor, A. Corma, P. Jones, L. Villaescusa, *J. Phys. Chem.* **1998**, *102*, 4147-4155. 546
- 500 [5] Z. Qin, L. Lakiss, L. Tosheva, J.-P. Gilson, A. Vicente, C. Fernandez, V. Valtchev, *Adv. Funct. Mater.* **2014**, *24*, 257-264. 547
- 501 [6] R. M. Barrer, *Hydrothermal chemistry of zeolites*, Academic press, **1982**. 548
- 502 [7] R. M. Milton, *Molecular sieve science and technology: a historical perspective*. ACS Publications, Eds. M. L. Occelli & H. E. Robson, 1989, pp. 1-10. 549
- 503 [8] D. W. Breck, *Zeolite molecular sieves: structure, chemistry and use*, Wiley, New York, **1974**. 550
- 504 [9] E. M. Flanigen, R. L. Patton, United States Patent, No. 4073865, **1978**. 551
- 505 [10] a) J. Guth, H. Kessler, J. Higel, J. Lamblin, J. Patarin, A. Seive, J. Chezeau, R. Wey, ACS Publications, **1989**, pp. 176-195; b) J. Guth, H. Kessler, P. Caullet, J. Hazm, A. Merrouche, J. Patarin, in *Proceedings from the Ninth International Zeolite Conference*, Elsevier, **1993**, pp. 215-222; c) J. Guth, H. Kessler, R. Wey, in *Studies in Surface Science and Catalysis, Vol. 28*, Elsevier, **1986**, pp. 121-128. 552
- 506 [11] P. Caullet, J.-L. Paillaud, A. Simon-Masseron, M. Soulard, J. Patarin, *Comptes Rendus Chimie* **2005**, *8*, 245-266. 553
- 507 [12] B. Louis, L. Kiwi-Minsker, *Microporous Mesoporous Mater.* **2004**, *74*, 171-178. 554
- 508 [13] F. Ngoye, L. Lakiss, Z. Qin, S. Laforge, C. Canaff, M. Tarighi, V. Valtchev, K. Thomas, A. Vicente, J. P. Gilson, Y. Pouilloux, C. Fernandez, L. Pinard, *J. Catal.* **2014**, *320*, 118-126. 555
- 509 [14] V. Eroshenko, R.-C. Regis, M. Soulard, J. Patarin, *J. Am. Chem. Soc.* **2001**, *123*, 8129-8130. 556
- 510 [15] a) F. L. Bleken, S. Chavan, U. Olsbye, M. Boltz, F. Ocampo, B. Louis, *Applied Catalysis A: General* **2012**, *447-448*, 178-185; b) O. Larlus, V. P. Valtchev, *Chem. Mater.* **2005**, *17*, 881-886. 557
- 511 [16] C. A. Fyfe, D. H. Brouwer, A. R. Lewis, J.-M. Chezeau, *J. Am. Chem. Soc.* **2001**, *123*, 6882-6891. 558
- 512 [17] a) O. B. Ayodele, H. F. Abbas, W. Daud, *Energy Conv. Manag.* **2014**, *88*, 1111-1119; b) C. I. Round, C. D. Williams, K. Latham, C. V. Duke, *Chem. Mater.* **2001**, *13*, 468-472. 559
- 513 [18] S. Mintova, V. Valtchev, *Microporous Mesoporous Mater.* **2002**, *55*, 171-179. 560
- 514 [19] J. Antonio Alves Júnior, J. Baptista Baldo, *New Journal of Glass and Ceramics* **2014**, *04*, 29-37. 561
- 515 [20] K. Gayer, L. Thompson, O. Zajicek, *Can. J. Chem.* **1958**, *36*, 1268-1271. 562
- 516 [21] H. Koller, A. Wölker, L. Villaescusa, M. Diaz-Cabanas, S. Valencia, M. Cambor, *J. Am. Chem. Soc.* **1999**, *121*, 3368-3376. 563
- 517 [22] K. A. Cychoz, R. Guillet-Nicolas, J. Garcia-Martinez, M. Thommes, *Chem. Soc. Rev.* **2017**, *46*, 389-414. 564

- 580 [23] a) U. Müller, K. Unger, in *Studies in*
581 *Surface Science and Catalysis, Vol. 39,*
582 Elsevier, **1988**, pp. 101-108; b) K. Nakai,
583 J. Sonoda, M. Yoshida, M. Hakuman, H.
584 Naono, *Adsorption* **2007**, *13*, 351-356.
- 585 [24] J. Parra, C. Ania, D. Dubbeldam, T. Vlugt,
586 J. Castillo, P. Merklings, S. Calero, *J. Phys.*
587 *Chem. C* **2008**, *112*, 9976-9979.
- 588

589
590
591
592

Entry for the Table of Contents



593
594
595
596
597
598

This paper deals with the zeolite synthesis in acidic medium. The isoelectric point of silica source is found to be the critical factor controlling the zeolite formation under acidic conditions. The zeolite crystallizes solely at pH above the IEP when the silica particles are negatively charged.